Electronic Supplementary Material (ESI) for Nanoscale.

SUPPLEMENTAL INFORMATION

Self-Powered Ion Detectors Based on Dye-Sensitized Photovoltaics

AUTHORS: *Kanika L. Agrawal and Max Shtein*[*]

Materials Science and Engineering
University of Michigan, Ann Arbor, MI 48109

---

[*] *mshtein@umich.edu*

Methods

Device Fabrication: 8 - 9 µM thick transparent TiO_2 films were prepared by doctor blading commercially available Ti-Nanoxide T/SP paste (Solaronix Inc.) on 2.2 mm thick fluorine doped tin oxide with a sheet resistance of 7 ohm/square. The substrates were cleaned using organic solvents and pre-treated in 40 mM aqueous $TiCl_4$ solution at 70 ^{0}C for 30 minutes prior to film deposition. After coating with TiO_2 paste, the substrates were fired for 30 minutes at 450 ^{0}C to allow a porous nanocrystalline film to form. *(see Supplementary Fig. 6*) This step was followed up with a $TiCl_4$ post-treatment and additional sintering at 450 ^{0}C for 15 minutes. The prepared films were allowed to cool down to approximately 50 ^{0}C and immersed in a 0.5 mM solution of commercial N3 dye (Sigma Aldrich). The dye solution was prepared by dissolving N3 in an 8/2 (v/v) mixture of tetrahydrofuran and t-butanol. The films were soaked in dye solution for 24 hours after which they were removed from solution, rinsed with isopropanol and dried under a stream of compressed N_2. For device assembly, a 25 µM Surlyn gasket (Solaronix, Inc.) was placed between the working electrode and the counter electrode following which, the device was placed on a hotplate at 100 ^{0}C and pressed down on for ~ 30 seconds to ensure a good seal is obtained. The counter electrode was prepared by sputtering 50 nm Pt on FTO. Additionally, screen printed TiO_2 films consisting of a 10 µM transparent film of 15 - 20 nm diameter particles followed by a 3 - 4 µM scattering layer of 400 nm diameter particles obtained from Solaronix Inc. were also tested. *(see Supplementary Fig. 7*)

Electrolyte & Analyte Preparation: Electrolyte solutions were introduced into the device through a 0.5 mm diameter drilled hole in the counter electrode using a Vac'n'Fill syringe (Solaronix, Inc.). The ideal electrolyte solution contained 0.6 M 1,2-dimethyl-3-propylimidazolium iodide (DMPII), 0.1 M Lithium Iodide (LiI), 0.05 M Iodine (I_2) and 0.5 M 4-tert-butylpyridine (tBP) in acetonitrile. Analyte solutions were prepared by dissolving $AgNO_3$ concentrations ranging from 1 nM to 1 mM in acetonitrile.

Solar Cell Characterization: Current-Voltage (JV) characteristics were recorded using a Solartron Analytical Modulab MTS Materials Test System. The cells were illuminated with a Newport solar simulator (model# 91191- 1000) calibrated to AM1.5 (100 mW/cm^2) using an NREL Si reference cell (Model PVM233 KG5).

Electrochemical Impedance Spectroscopy: EIS measurements were recorded using the Solartron Analytical Modulab MTS Materials Test System. The cells were scanned over a frequency range of 100 kHz to 0.1 Hz with 10 mV amplitude, at open-circuit conditions, under 1 sun illumination. The obtained Nyquist plots were fit using an equivalent circuit model to extract relevant parameters.

Energy Dispersive X-ray Spectroscopy: SEM and EDS measurements were made using a Hitachi SU8000 scanning electron microscope. The spectra and images shown in Figure 5 were obtained by applying an acceleration voltage of 10 kV and a working distance of 15.3 mm.

Fitting electrochemical impedance spectroscopy (EIS) data:

A sample of the data obtained from EIS measurements is shown below along with the definition of each internal resistance identified. Since our data does not show a distinct semi-circle corresponding to the low-frequency resistance R_D, typically arising from electrolyte diffusion, we do not include this parameter in our model. The fits were performed using ZView software (Solartron Analytical). Here, R_{FTO} corresponds to the sheet resistance of the fluorine doped tin oxide (FTO) substrate, R_R is the resistance corresponding to recombination at the TiO_2/dye/electrolyte interface, R_{CT} is the resistance to charge transfer at the counter electrode and CPE1 and 2 are constant phase elements.

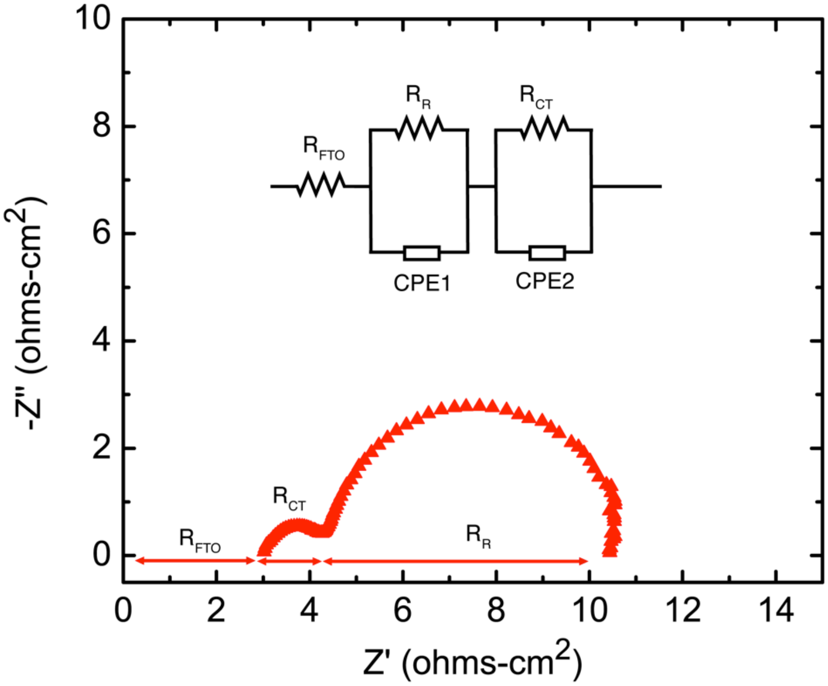

Fig. 1. EIS data of a typical device under AM 1.5 (100 mW/cm^2) simulated sunlight at open-circuit conditions. Shown here are the resistances corresponding to the high, mid and low-frequency regions on the Nyquist plot. *Inset:* Equivalent circuit model used to fit the data.

Modeling device current density-voltage (JV) characteristics:

To model the JV characteristics of the system, we consider a modified equivalent circuit model as described by Han et al. [1]

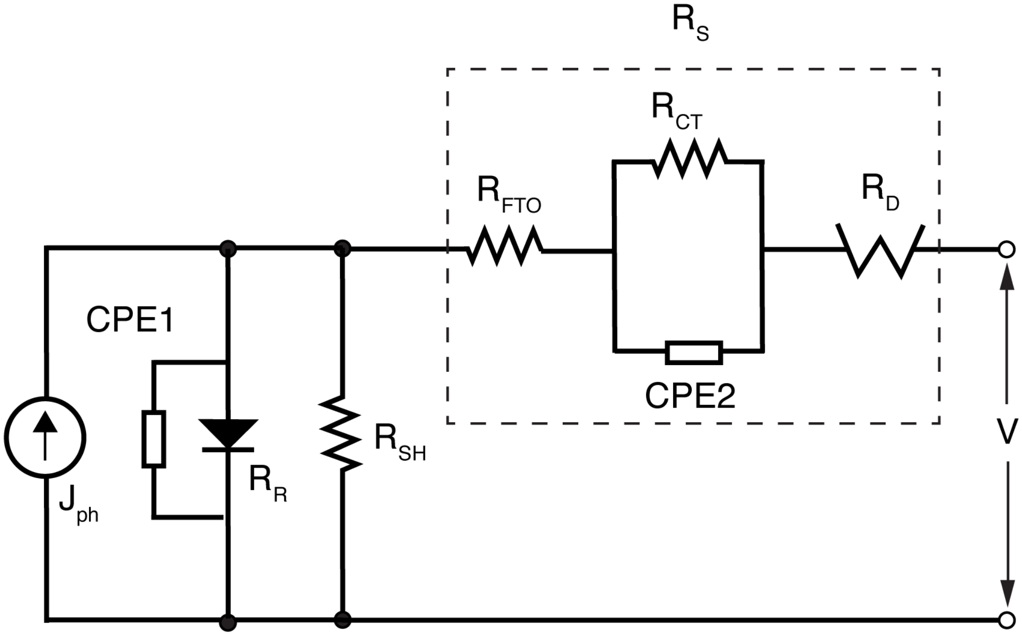

Fig. 2. Here, J_{ph} is the photocurrent, R_S is the series resistance, R_{SH} is the shunt resistance, and V is the bias voltage, while R_{FTO} corresponds to the sheet resistance of the FTO, R_R is the resistance corresponding to recombination at the TiO_2/dye/electrolyte interface, R_{CT} is the resistance to charge transfer at the counter electrode, R_D (Warburg element) corresponds to the electrolyte diffusion resistance and CPE1 and 2 are constant phase elements.

For JV modeling, the capacitances associated with R_R and R_{CT} may be ignored since these measurements are performed under DC conditions, while R_R may be treated as a diode. We lump the other three internal resistances into one fitting parameter $'R_S'$. The JV curve can now be modeled as per the generalized Shockley equation. [2].

$$J = \frac{R_{SH}}{R_S + R_{SH}} \left\{ J_S \left[\exp\left(\frac{q(V - JR_S)}{nkT} \right) - 1 \right] + \frac{V}{R_{SH}} \right\} - J_{ph}(V)$$

where J_S is the reverse dark saturation current and n is the ideality factor. To obtain the trends seen in Fig. 4, we set $J_{ph} = J_{SC}$ and R_{SH} = 0.1 MΩ- cm^2 (estimated from dark current data) with R_S, J_S, and n as fitting parameters.

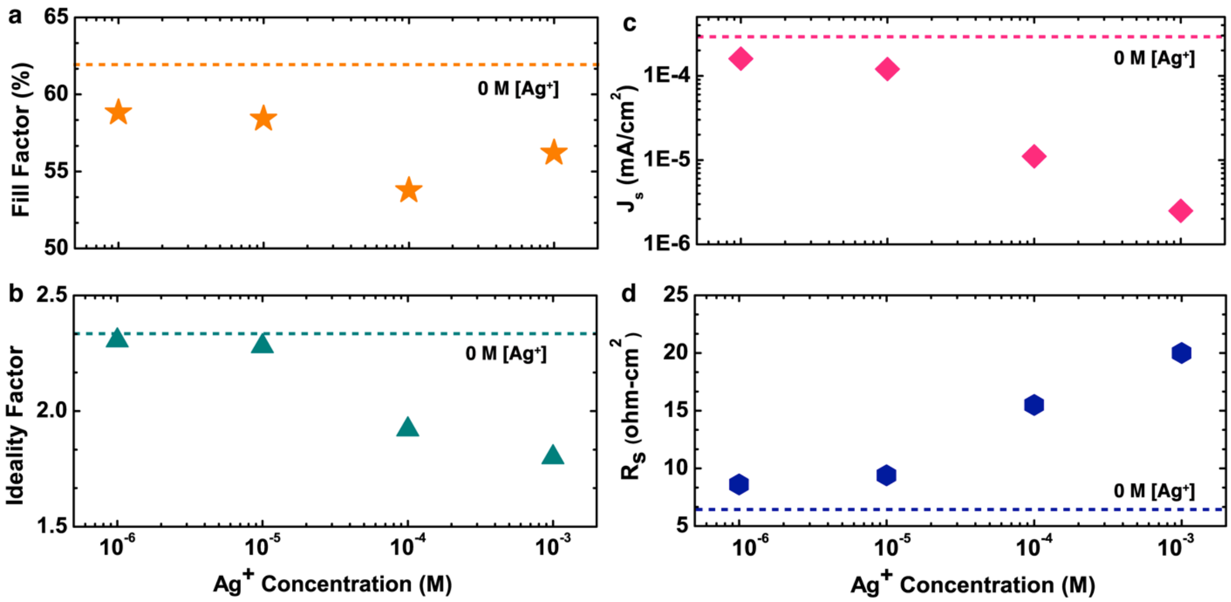

Fig. 3. **(a)** Changes in fill factor as a function of [Ag$^+$]. No noticeable trend is seen here **(b)** The ideality factor (n) obtained from fitting our data to a Shockley model as a function of [Ag$^+$]. **(c)** Changes in the saturation current in the dark plotted as a function of [Ag$^+$]. **(d)** Changes in series resistance plotted as a function of [Ag$^+$].

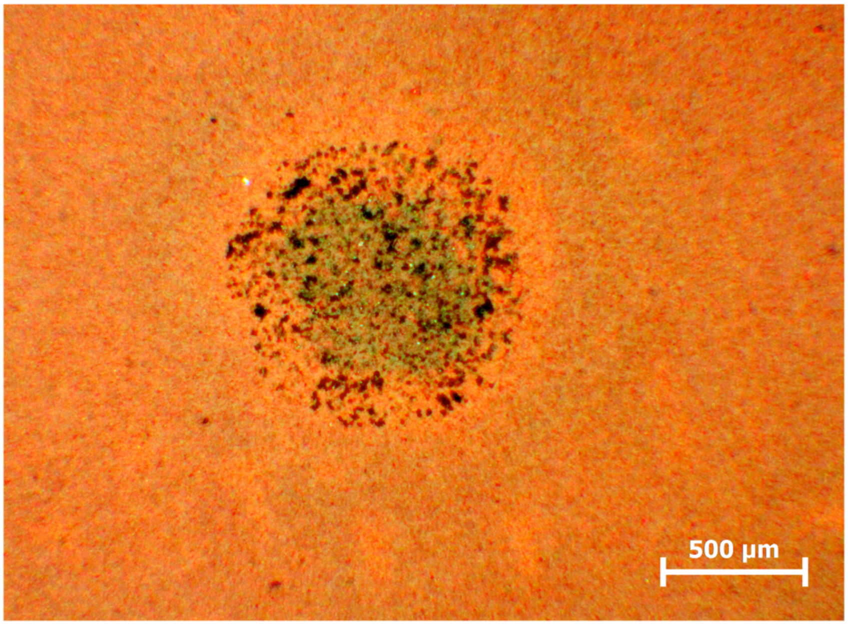

Fig. 4. An image showing silver clusters formed on the TiO_2 film after sensor tests were performed, directly underneath the filling hole.

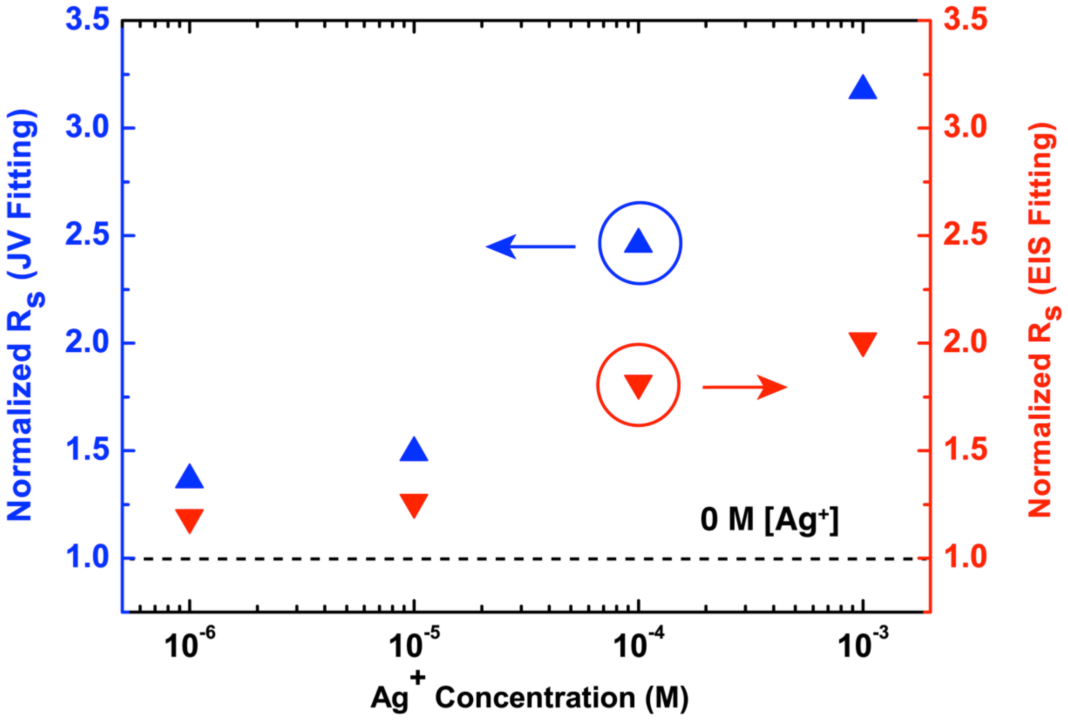

Fig. 5. The left hand side y-axis shows the normalized values of R_S that are obtained from fitting the JV data to a Shockley model as seen in Fig. 4(d). The right-hand side y-axis shows the normalized values of R_S that are obtained by plugging in the resistance values obtained from EIS measurements into the following equation: $R_S = R_{FTO} + R_{CT}$. It must be noted that R_D was not taken into account, since we could not fit this resistance, as previously mentioned. The discrepancy between the two sets of R_S values, especially at higher concentrations of Ag^+ most likely arises from this omission. Consequently, it appears that R_D becomes larger at higher concentrations of Ag^+, which is consistent with the hypothesis that the mobility of triiodide ions is reduced as the Ag^+ content in the electrolyte becomes larger.

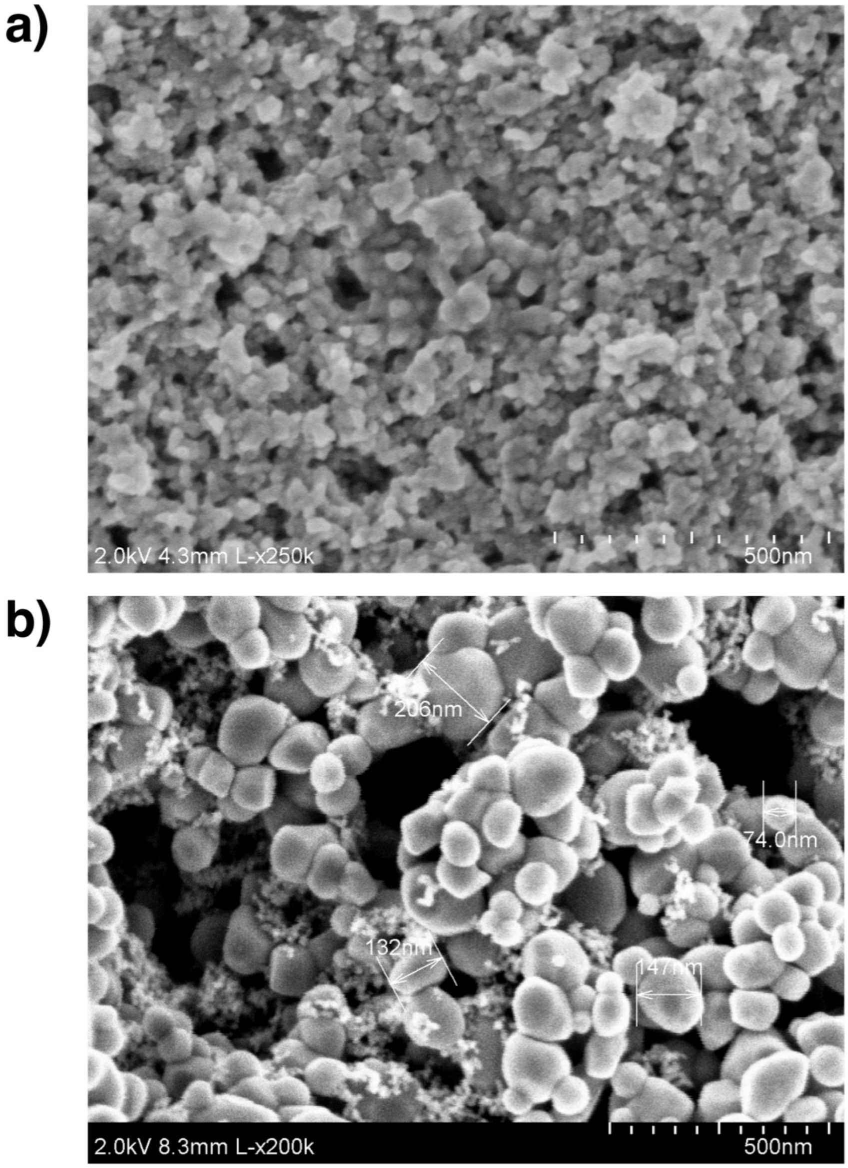

Fig. 6. **(a)** An SEM image of a TiO_2 electrode prepared by doctor blading 9 μM thick film of T/SP paste. **(b)** SEM image of a screen printed TiO_2 electrode consisting a 10 μM transparent film of 15 - 20 nm diameter particles followed by a 3 - 4 μM scattering layer of 400 nm diameter particles obtained from Solaronix Inc.

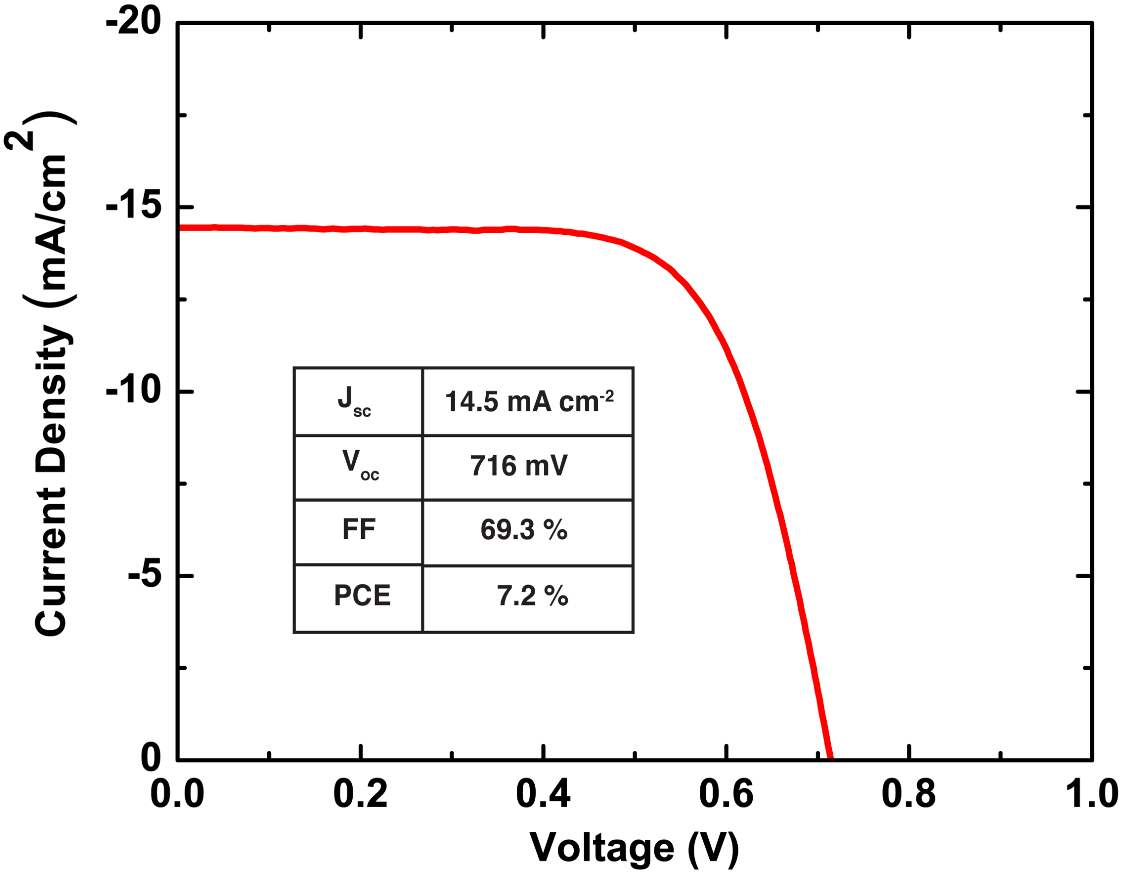

J_{sc}	14.5 mA cm^{-2}
V_{oc}	716 mV
FF	69.3 %
PCE	7.2 %

Fig. 7. J-V characteristics of a device with a screen-printed TiO_2 electrode (transparent + scattering films) under AM 1.5 (100 mW/cm^2) simulated sunlight. The area of the dye coated TiO_2 region was 0.36 cm^2. *Inset:* Obtained performance parameters for one such device. Based on literature, the scattering layer should facilitate a current enhancement by increasing light absorption within the device. However, we did not find such an improvement to occur perhaps because the screen-printed films were not freshly prepared.

Notes and references

1. L. Han, N. Koide, Y. Chiba and T. Mitate, *App. Phys. Lett.* 2004, **84**, 2433.
2. R. H. Bube and A. L. Fahrenbruch, *Advances in Electronics and Electron Physics* (Academic, New York, 1981), p. 163.